Zilch vortical effect

M. N. Chernodub,[1,2] Alberto Cortijo,[3] and Karl Landsteiner[4]

[1] *Institut Denis Poisson UMR 7013, Université de Tours, 37200 Tours, France*
[2] *Laboratory of Physics of Living Matter, Far Eastern Federal University, Sukhanova 8, Vladivostok 690950, Russia*
[3] *Materials Science Factory, Instituto de Ciencia de Materiales de Madrid, CSIC, Cantoblanco, 28049 Madrid, Spain*
[4] *Instituto de Física Teórica UAM/CSIC, C/ Nicolás Cabrera 13-15, Cantoblanco, 28049 Madrid, Spain*

(Received 18 August 2018; published 27 September 2018)

We study the question of whether a helicity-transporting current is generated in a rotating photon gas at finite temperature. One problem is that there is no gauge-invariant local notion of helicity or helicity current. We circumvent this by studying not only the optical helicity current but also the gauge-invariant "zilch" current. In order to avoid problems of causality, we quantize the system on a cylinder of finite radius and then discuss the limit of infinite radius. We find that net helicity and zilch currents are only generated in the case of the finite radius and are due to duality-violating boundary conditions. A universal result exists for the current density on the axes of rotation in the high-temperature limit. To lowest order in the angular velocity, it takes a form similar to the well-known temperature dependence of the chiral vortical effect for chiral fermions. We briefly discuss possible relations to gravitational anomalies.

DOI: 10.1103/PhysRevD.98.065016

I. INTRODUCTION

The quantum field theory of chiral fermions predicts a number of exotic transport phenomena such as the generation of a current in a magnetic field or under rotation. These are known as chiral magnetic and chiral vortical effects (see Refs. [1,2] for recent reviews). Both effects are related to the presence of chiral anomalies. In particular, the chiral vortical effect (CVE) is present at finite temperature and can be understood as a signal of (possibly global) mixed gravitational anomalies [3–11].

From the outset it should be emphasized that in a relativistic theory rotation cannot be implemented by simply introducing a constant angular velocity in a thermal ensemble [12]. In infinite space there appears necessarily a region in which the tangential velocity would exceed the speed of light. There are two remedies to this. In a hydrodynamic setup one can consider either localized vortices in the fluid or, alternatively, one can restrict the ensemble to a finite space-time region in which no superluminal velocities arise. In infinite space the CVE can be computed by studying an ensemble of rotating fermions and concentrating on the region at the center of rotation [12]. Alternatively one can study an ensemble confined within the boundaries of a rotating cylinder [13–18].

Recently, the question has arisen of if and how a similar effect for ensembles of rotating photons could be made possible [19–21]. In part, this question can be motivated by the relation of the CVE to the mixed gravitational anomalies as well as by the interesting results on the existence of a similar anomaly for photons [22,23]. At first sight, in the case of photons the notion of chirality could naturally be replaced by the concept of helicity. It turns out, however, that the definition of a photonic helicity current analogous to a fermionic chiral (or axial) current is much more subtle. A standard way of defining a photonic helicity current is the so-called magnetic helicity, which in covariant notation can be written as

$$J^{\mu}_{mh} = \epsilon^{\mu\nu\rho\lambda} A_{\nu} F_{\rho\lambda}. \tag{1}$$

The drawback of this way of defining helicity is that the current (1) is neither conserved (since $\partial_\mu J^{\mu}_{mh} = \tilde{F}^{\mu\nu} F_{\mu\nu}$ with $\tilde{F}^{\mu\nu} = \frac{1}{2}\epsilon^{\mu\nu\rho\lambda} F_{\rho\lambda}$) nor gauge invariant. The first inconvenience can be remedied by also defining the so-called "optical helicity" [24]

$$J^{\mu}_{h} = \frac{1}{2}\epsilon^{\mu\nu\rho\lambda}(A_{\nu} F_{\rho\lambda} - C_{\nu} \tilde{F}_{\rho\lambda}), \tag{2}$$

where C_μ is a dual gauge potential defined via the relation $\tilde{F}_{\mu\nu} = \partial_\mu C_\nu - \partial_\nu C_\mu$. This current is conserved, $\partial_\mu J^{\mu}_{h} = 0$, but now there is a new inconvenience: the original A_μ and dual C_μ gauge fields are not locally related to each other. As long as one does not insist on a Lorentz-invariant Lagrangian formulation of Maxwell's equations that might not be considered a fundamental problem. However the optical helicity is still not gauge invariant and now there are even two gauge symmetries since $C'_\mu = C_\mu + \partial_\mu \theta$ and C_μ are physically equivalent dual gauge potentials. A gauge-invariant global helicity charge $\mathcal{Q} = \int d^3x J_h^0$ can still be defined, but there is no covariant expression for the helicity density which could be local in terms of the original A_μ and dual C_μ potential and gauge invariant with respect to both the original and dual gauge transformations.

Fortunately, there are other candidates for physically meaningful measures of helicity. Quite some time ago Lipkin pointed out that the free Maxwell theory allows for an additional conserved quantity [25] and soon afterwards Kibble noticed that due to the fact that it is a noninteracting theory there is, in fact, an infinite number of such conserved charges [26]. Following the nomenclature introduced by Lipkin these charges are known as "zilches." For monochromatic light, there is a relation between Lipkin's original zilch and the optical helicity [27], although they are quantities with different properties: while the optical helicity is the generator of the electric-magnetic duality transformations [28], the zilch generates a more complex transformation, involving extra derivatives [29].

The zilches are (classically) conserved quantities which, except for the optical helicity, have unusual dimensions. We will consider here only the original zilch introduced by Lipkin, a conserved current of dimension five. While a physical interpretation of the zilch remained obscure for a long time, recently it was shown that the zilch measures the asymmetry in the interaction of the electromagnetic field with small chiral molecules [30] similarly to the effects of the optical helicity on chiral and magnetoelectric media [31,32] and Weyl semimetals [33]. We therefore take the zilch as a legitimate local measure of the helicity of light.

In order to study the possible realization of a version of the chiral vortical effect for photons we will quantize Maxwell theory on a finite cylinder of radius R and consider an ensemble with a finite fixed angular velocity such that $|\Omega R| < 1$. We calculate the thermal averages for the optical helicity current and zilch current along the direction of rotation and study the infinite-space limit $R \to \infty$. It turns out that this infinite-space limit is—in contrast to the fermionic case—ill defined even if one concentrates on the current at the center of rotation. For finite radius and $|\Omega R| < 1$ the ensemble is well defined but the appearance of a nonvanishing total current depends very sensitively on the boundary conditions.

We will study three types of boundary conditions: a perfect electric conducting boundary, a perfect magnetic conducting boundary and duality-invariant unbounded space. Our finding is that the integrated helicity and zilch currents vanish exactly in the duality-invariant case whereas only one type of polarization leads to a nonvanishing net current in the other two cases. More precisely, the Dirichlet boundary conditions on the photon wave functions lead to exactly vanishing net current and only Neumann boundary conditions give rise to a net current. However, the perfect conducting and dual conducting boundary conditions break the electric-magnetic duality and therefore introduce a source of helicity or zilch on the boundary. We interpret the net current therefore not as an intrinsic chiral vortical effect but as a result of the symmetry-breaking boundary conditions.

This work is organized as follows. In Sec. II we introduce our notation, the (non-Lorentz-covariant) versions of helicity and zilch and associated currents. Then we quantize the Maxwell field in the Coulomb gauge on a cylinder of radius R. In Sec. III we study the helicity, zilch and energy currents. We show that the net currents integrated over a cross section of the cylinder vanish for the Dirichlet boundary conditions on radial functions of photons. We numerically evaluate the thermal current distributions for different temperatures and angular velocities. Finally, we study the infinite-space limit and show that in this limit the current at the axis of rotation is a mathematically ill-defined quantity. Indeed, if one tries to evaluate it by an analytic continuation (using inversion relations for polylogarithms) then one finds a complex result. While a truncation to lowest order in angular velocity does give a finite expression it does not coincide with the results previously reported in the literature for the photonic CVE.

In any case, the physical significance of such a finite result for the photonic CVE is questionable since the resulting integrals for the thermal averages are mathematically well defined only in the strict case $|\Omega| + \epsilon = 1/R$ with $\epsilon > 0$. This requirement means that the zero-rotation limit, $\Omega \to 0$, should precede the infinite-volume limit $R \to \infty$. We emphasize that this requirement sets a stronger constraint for the rotating photons as compared to the case for fermions, because it arises from the essential property of bosons that the Bose-Einstein distribution function can take negative values for effectively negative energies, signaling a possible instability towards condensation of low-energy modes. Despite the difficulties with the calculation in the unbounded domain we find numerically that the high-temperature limit of the central current density in the bounded domain does converge to the result in the unbounded domain at linear order in the angular velocity.

We present our conclusions in Sec. IV. Some of our conventions for vector analysis and useful properties of the Bessel functions are given in the Appendices.

II. PHOTONS IN A NONROTATING CYLINDER

We consider a thermalized photon gas at a fixed temperature T in an infinitely long straight cylindrical volume (often called a "waveguide" in the literature). The cylinder has a fixed finite radius R and may rotate around its symmetry axis with constant angular velocity Ω. For the sake of simplicity we work in vacuum with permittivity $\varepsilon = 1$ and permeability $\mu = 1$. We also set the speed of light and the reduced Planck constant to unity, $c = \hbar = 1$.

A. System of equations

1. Maxwell's equations

The electromagnetic fields are described by Maxwell's equations,

$$\nabla \cdot \boldsymbol{E} = 0, \tag{3a}$$

$$\nabla \cdot \boldsymbol{B} = 0, \tag{3b}$$

$$\nabla \times \boldsymbol{B} - \frac{\partial \boldsymbol{E}}{\partial t} = 0, \tag{3c}$$

$$\nabla \times \boldsymbol{E} + \frac{\partial \boldsymbol{B}}{\partial t} = 0, \tag{3d}$$

where the magnetic field $\boldsymbol{B}$ and the electric field $\boldsymbol{E}$ are related to the gauge potential $A^\mu = (\phi, \boldsymbol{A})$ as follows:

$$\boldsymbol{B} = \nabla \times \boldsymbol{A}, \qquad \boldsymbol{E} = -\nabla\phi - \frac{\partial \boldsymbol{A}}{\partial t}. \tag{4}$$

To solve these equations inside a cylinder it is natural to introduce cylindrical coordinates with the radius ρ, the azimuthal angle φ, the height z, and the time coordinate t (in the laboratory reference frame). Certain useful formulas of vector calculus in the cylindrical system of coordinates are summarized in Appendix A.

Given the geometry of the problem and the linearity of Maxwell's equations the solutions can be described in the complexified form

$$\boldsymbol{G}(\rho, \varphi, z, t) = e^{-i\omega t + im\varphi + ik_z z}\boldsymbol{G}(\rho), \tag{5}$$

where $\boldsymbol{G} = \boldsymbol{E}, \boldsymbol{B}, \boldsymbol{A}$ are the positive-frequency solutions for the electromagnetic fields with energy $\omega \geq 0$, momentum k_z along the z axis, and quantized angular number $m \in \mathbb{Z}$, corresponding to the eigenvalue of angular momentum about the z axis. In Eq. (5) the radial functions $\boldsymbol{G}(\rho)$ are determined by Maxwell's equations (A3) and by the boundary conditions that will be specified below.

2. Boundary conditions

The spectrum of solutions of Maxwell's equations (A3) depends on the type of boundary conditions at the edge of the cylinder at a fixed radial coordinate $\rho = R$. We will consider three kinds of boundary conditions, corresponding to a boundary made of (i) a perfect electric conductor (an ideal metal), (ii) its "dual" analogue, a perfect magnetic conductor and finally (iii) duality-invariant "natural" boundary conditions in infinite space.

We will study an ensemble of rotating photons in a fixed laboratory frame. That means we should have energy and angular momentum as conserved charges to which we can couple corresponding Lagrange multipliers, the temperature T and the angular velocity Ω to define a grand canonical ensemble.

For the Maxwell field the energy and momentum conservation take the form

$$\frac{\partial \epsilon}{\partial t} + \nabla \cdot \boldsymbol{P} = 0, \qquad \frac{\partial P_l}{\partial t} + \nabla_m \sigma^m{}_l = 0, \tag{6}$$

where the energy, momentum density (Poynting vector) and stress tensor are, respectively,

$$\epsilon = \frac{1}{2}(\boldsymbol{E}^2 + \boldsymbol{B}^2), \tag{7}$$

$$\boldsymbol{P} = \boldsymbol{E} \times \boldsymbol{B}, \tag{8}$$

$$\sigma_{ml} = -E_m E_l - B_m B_l + \frac{1}{2} g_{ml}(\boldsymbol{E}^2 + \boldsymbol{B}^2). \tag{9}$$

Here $\boldsymbol{A} \cdot \boldsymbol{B} \equiv \sum_{l=1}^{3} A_l B_l$ is the scalar product and $l, m = 1, 2, 3$ are the spatial indices.

In cylindrical geometry the globally conserved quantities are the energy ϵ, the momentum along the cylinder axis P_z and the z component of the angular momentum $L_z \equiv (\boldsymbol{\rho} \times \boldsymbol{P})_z = \rho P_\varphi$. Because we require the boundary of the cylinder to respect the conservation of these quantities, Eq. (6) implies that these quantities are conserved provided both the radial component of the Pointing vector (8) and the radial components of the photon stress tensor (9) vanish at $\rho = R$:

$$\begin{aligned} P_\rho(R) &= E_\varphi(R) B_z(R) - E_z(R) B_\varphi(R) = 0, \\ \sigma_{\rho\varphi}(R) &= -E_\rho(R) E_\varphi(R) - B_\rho(R) B_\varphi(R) = 0, \\ \sigma_{\rho z}(R) &= -E_\rho(R) E_z(R) - B_\rho(R) B_z(R) = 0. \end{aligned} \tag{10}$$

Therefore one may distinguish three types of boundary conditions.

(i) Ideal electric conductor: An external electromagnetic field generates dissipationless electric currents in an ideal electric conductor that lead to a vanishing normal component (with respect to the surface element ∂S of the conductor) of the external magnetic field $B_\perp$ and two tangential components $\boldsymbol{E}_\parallel$ of the electric field at the surface boundary:

$$B_\perp|_{x \in S} = 0, \qquad \boldsymbol{E}_\parallel|_{x \in S} = 0. \tag{11}$$

In cylindrical coordinates the boundary conditions imposed by the perfect electric conductor (11) have the following form:

$$B_\rho(R) = E_z(R) = E_\varphi(R) = 0. \qquad (12)$$

These conditions ensure conservation of energy as well as the z components of momentum and angular momentum (10).

(ii) Ideal magnetic conductor as a dual analogue of the ideal electric conductor: Instead of electric currents, a perfect magnetic conductor hosts dissipationless magnetic currents.[1] The magnetic boundary conditions are therefore dual to the electric ones (11):

$$E_\perp|_{x\in S} = 0, \qquad \boldsymbol{B}_\parallel|_{x\in S} = 0. \qquad (13)$$

The magnetic conductor (13) imposes the following conditions on the electromagnetic fields which ensure the physical constraints (10):

$$E_\rho(R) = B_z(R) = B_\varphi(R) = 0. \qquad (14)$$

One can readily observe that the perfect electric conductor or perfect magnetic conductor impose the conditions (12) and (14), which are mutually "dual" to each other. These boundary conditions will impose either Dirichlet or Neumann boundary conditions on a scalar radial function of the photon field depending on its polarization. The electromagnetic duality transformation

$$\boldsymbol{E} \to -\boldsymbol{B}, \qquad \boldsymbol{B} \to \boldsymbol{E}, \qquad (15)$$

exchanges the boundary conditions between the two possible polarizations.

(iii) Unbounded flat space: This is the limit $R \to \infty$. We impose "natural" boundary conditions by requiring that the fields and their products be integrable with the measure $\int_0^\infty \rho d\rho$. These fields can be represented by a Fourier-Bessel integral. In principle, the basis of eigenfunctions for both previously considered boundary conditions can also be used for the unbounded flat space. However it turns out that it is slightly more convenient to introduce in this case an explicitly helicity-preserving basis in terms of left- and right-circularly polarized photon wave functions.

B. Solutions

1. Quantization and normalization of electromagnetic fields

It is convenient to characterize the photon solutions in the interior of the cylinder by transverse electric and transverse magnetic polarization modes. The transverse electric (TE) mode possesses the electric field which is always perpendicular to the axis of the cylinder, $E_z^{\mathrm{TE}} = 0$. In the transverse magnetic (TM) mode it is the magnetic field that is perpendicular to the cylinder's axis, $B_z^{\mathrm{TE}} = 0$.

For the quantization of the gauge field it is convenient to choose the Coulomb gauge, where the temporal component of the gauge field is zero and the spatial part of the gauge field has zero divergence:

$$A_0(x) = 0, \qquad \boldsymbol{\nabla}\cdot\boldsymbol{A}(x) = 0. \qquad (16)$$

Then the photon operator is given by

$$\hat{\boldsymbol{A}}_\mu(x) = \sum_{J,\lambda} \frac{\boldsymbol{\epsilon}_J^{(\lambda)}}{\sqrt{2\omega_J}} (\mathcal{A}_J^{(\lambda)}(x)\hat{a}_J^{(\lambda)} + \mathcal{A}_J^{(\lambda),*}(x)\hat{a}_J^{(\lambda)\dagger}), \qquad (17)$$

where $\lambda = \mathrm{TE}, \mathrm{TM}$ is the polarization of the photon field and J is a collective notation for other quantum numbers which will be defined below.

In Eq. (17) the operators $\hat{a}_J^{(\lambda)}$ and $\hat{a}_J^{(\lambda)\dagger}$ annihilate and, respectively, create a photon with polarization λ, quantum number J, and wave function $\mathcal{A}_{J,\mu}^{(\lambda)}$. These operators obey the standard set of bosonic commutation relations:

$$\left[\hat{a}_J^{(\lambda)}, \hat{a}_{J'}^{(\lambda')\dagger}\right] = \delta_{\lambda\lambda'}\delta_{JJ'}, \qquad (18a)$$

$$\left[\hat{a}_J^{(\lambda)}, \hat{a}_{J'}^{(\lambda')}\right] = \left[\hat{a}_J^{(\lambda)\dagger}, \hat{a}_{J'}^{(\lambda')\dagger}\right] = 0, \qquad (18b)$$

where $\delta_{JJ'}$ is an identity in the phase space of quantum numbers J with the natural property

$$\sum_J \delta_{JJ'} = 1 \quad \text{for any } J'. \qquad (19)$$

The photonic vacuum state is annihilated by the operators $\hat{a}_J^{(\lambda)}$ for all λ and J:

$$\hat{a}_J^{(\lambda)}|0\rangle = 0. \qquad (20)$$

The photon wave functions with a definite polarization λ

$$\boldsymbol{\mathcal{A}}_J^{(\lambda)} = \boldsymbol{\epsilon}_J^{(\lambda)}\mathcal{A}_J^{(\lambda)}, \qquad (21)$$

are defined by the orthonormal vectors

$$\boldsymbol{\epsilon}_J^{(\lambda)}\cdot\boldsymbol{\epsilon}_J^{(\lambda')} = \delta_{\lambda\lambda'}, \qquad \lambda = \mathrm{TE}, \mathrm{TM}, \qquad (22)$$

for each fixed quantum number J. For a fixed polarization λ, the expansion coefficients of the photon operator (17) are orthonormalized according to the condition

$$\int d^3x \mathcal{A}_J^{(\lambda)*}(\boldsymbol{x})\mathcal{A}_{J'}^{(\lambda)}(\boldsymbol{x}) = \delta_{JJ'}. \qquad (23)$$

In our conventions there are no sums over repeated indices [e.g., over the cumulative index J in Eq. (21)] unless explicitly indicated.

[1]The perfect-magnetic boundary conditions can be viewed as the electromagnetic analogue of the boundary conditions for a gluonic field in the MIT bag model for hadrons in QCD.

2. Explicit solutions at finite radius

The (positive-frequency) expansion coefficients of the photon operator (17) may be represented as follows:

$$\mathcal{A}^{(\lambda)}(\rho,\varphi,z,t) = e^{-i\omega t + ik_z z + im\varphi}\mathcal{A}^{(\lambda)}(\rho), \tag{24}$$

where

$$\omega = \sqrt{k_z^2 + k_\perp^2}, \tag{25}$$

is the frequency of the mode, k_z is the momentum along the axis of the cylinder and $m \in \mathbb{Z}$ is the quantum angular momentum associated with the angular rotations about the z axis. The quantization of the transverse (radial) momentum $k_\perp > 0$ in Eq. (25) depends on the boundary conditions at the edge of the cylinder.

In cylindrical coordinates, $\boldsymbol{A} \equiv (A_\rho, A_\varphi, A_z)^T$, the radial part of the wave function (24) is given, for the TE and TM polarizations, respectively, as

$$\mathcal{A}^{\mathrm{TE}}(\rho) = \begin{pmatrix} \frac{m f_{\mathrm{TE}}(\rho)}{i\rho} \\ \frac{\partial f_{\mathrm{TE}}(\rho)}{\partial\rho} \\ 0 \end{pmatrix}, \tag{26a}$$

$$\mathcal{A}^{\mathrm{TM}}(\rho) = \begin{pmatrix} \frac{k_z}{i\omega}\frac{\partial f_{\mathrm{TM}}(\rho)}{\partial\rho} \\ \frac{mk_z}{\omega}\frac{f_{\mathrm{TM}}(\rho)}{\rho} \\ -\frac{k_\perp^2}{\omega} f_{\mathrm{TM}}(\rho) \end{pmatrix}, \tag{26b}$$

where the scalar radial functions $f_\lambda = f_\lambda(\rho)$ obey the following differential equation ($\lambda = \mathrm{TE}, \mathrm{TM}$):

$$\frac{1}{\rho}\frac{\partial}{\partial\rho}\left(\rho\frac{\partial f_\lambda}{\partial\rho}\right) - \frac{m^2}{\rho^2} f_\lambda + k_\perp^2 f_\lambda = 0. \tag{27}$$

The normalized solutions of Eq. (27) are proportional to the Bessel functions of the first kind:

$$f_\lambda = C_\lambda J_m(k_\perp\rho), \qquad \lambda = \mathrm{TE}, \mathrm{TM}, \tag{28}$$

where C_λ are the normalization constants to be defined below.

In the Coulomb gauge the operators of electric and magnetic fields are given by a series similar to Eq. (17) where the expansion coefficients can be determined with the help of Eq. (4). The electric-field modes are proportional to the corresponding gauge field modes (26),

$$\mathcal{E}^{(\lambda)} = -\partial_t\mathcal{A}^{(\lambda)} = i\omega\mathcal{A}^{(\lambda)}, \tag{29}$$

while the magnetic-field modes $\mathcal{B}^{(\lambda)} = \boldsymbol{\nabla}\times\mathcal{A}^{(\lambda)}$ for the $\lambda = \mathrm{TE}, \mathrm{TM}$ polarizations are

$$\mathcal{B}^{\mathrm{TE}}(\rho) = \begin{pmatrix} -ik_z\frac{\partial f_{\mathrm{TE}}(\rho)}{\partial\rho} \\ mk_z\frac{f_{\mathrm{TE}}(\rho)}{\rho} \\ -k_\perp^2 f_{\mathrm{TE}}(\rho) \end{pmatrix}, \tag{30a}$$

$$\mathcal{B}^{\mathrm{TM}}(\rho) = \begin{pmatrix} -im\omega\frac{f_{\mathrm{TM}}(\rho)}{\rho} \\ \omega\frac{\partial f_{\mathrm{TM}}(\rho)}{\partial\rho} \\ 0 \end{pmatrix}. \tag{30b}$$

The cylinder made of an ideal electric conductor or a magnetic conductor imposes, respectively, the boundary conditions (12) or (14) on electromagnetic fields of the modes. These constraints can be rewritten as conditions on the radial functions of the corresponding electromagnetic modes:

$$\left.\frac{\partial f_{\mathrm{TE}}(\rho)}{\partial\rho}\right|_{\rho=R} = f_{\mathrm{TM}}(R) = 0, \qquad \mathfrak{b} = E, \tag{31a}$$

$$\left.\frac{\partial f_{\mathrm{TM}}(\rho)}{\partial\rho}\right|_{\rho=R} = f_{\mathrm{TE}}(R) = 0, \qquad \mathfrak{b} = M. \tag{31b}$$

For shortness, we call the boundary conditions corresponding to the perfect metal (12) and the perfect magnetic conductor (14) the "electric" ($\mathfrak{b} = E$) and "magnetic" ($\mathfrak{b} = M$) conditions, respectively. The duality of the electric and magnetic boundary conditions with respect to the TE and TM modes is clearly seen in Eq. (31).

The explicit form of the solutions (28) indicates that the boundary conditions (31) impose the following quantization of the radial momentum $k_\perp$ for the photon polarizations λ:

$$J'_m(k_\perp R) = 0, \qquad \begin{pmatrix}\lambda \\ \mathfrak{b}\end{pmatrix} = \begin{pmatrix}\mathrm{TE} \\ E\end{pmatrix}, \begin{pmatrix}\mathrm{TM} \\ M\end{pmatrix}, \tag{32}$$

$$J_m(k_\perp R) = 0, \qquad \begin{pmatrix}\lambda \\ \mathfrak{b}\end{pmatrix} = \begin{pmatrix}\mathrm{TE} \\ M\end{pmatrix}, \begin{pmatrix}\mathrm{TM} \\ E\end{pmatrix}, \tag{33}$$

where the prime indicates a derivative of the Bessel function with respect to its argument. Thus the walls of the cylinder made of a perfect electric ($\mathfrak{b} = E$) or magnetic ($\mathfrak{b} = M$) conductor quantize the transverse momentum $k_\perp$ of the TE and TM photon modes differently:

$$k_\perp^{\mathrm{TE}} = \frac{\kappa'_{ml}}{R}, \qquad k_\perp^{\mathrm{TM}} = \frac{\kappa_{ml}}{R}, \qquad \mathfrak{b} = E, \tag{34a}$$

$$k_\perp^{\mathrm{TE}} = \frac{\kappa_{ml}}{R}, \qquad k_\perp^{\mathrm{TM}} = \frac{\kappa'_{ml}}{R}, \qquad \mathfrak{b} = M, \tag{34b}$$

where κ_{ml} and κ'_{ml} (with $m \in \mathbb{Z}$) correspond to the lth positive root (with $l = 1, 2, \ldots \in \mathbb{N}$) of the Bessel function $J_m(x)$ and its derivative $J'_m(x)$, respectively,

$$J_m(\kappa_{ml}) = 0, \qquad J'_m(\kappa'_{ml}) = 0. \tag{35}$$

According to Eq. (25) the corresponding frequencies ω of the electromagnetic modes are

$$\omega_J = \sqrt{k_z^2 + \frac{(\kappa'_{ml})^2}{R^2}}, \qquad \begin{pmatrix} \lambda \\ \mathfrak{b} \end{pmatrix} = \begin{pmatrix} \mathrm{TE} \\ E \end{pmatrix}, \begin{pmatrix} \mathrm{TM} \\ M \end{pmatrix}, \tag{36a}$$

$$\omega_J = \sqrt{k_z^2 + \frac{(\kappa_{ml})^2}{R^2}}, \qquad \begin{pmatrix} \lambda \\ \mathfrak{b} \end{pmatrix} = \begin{pmatrix} \mathrm{TE} \\ M \end{pmatrix}, \begin{pmatrix} \mathrm{TM} \\ E \end{pmatrix}. \tag{36b}$$

In a cylinder the photonic modes of a definite polarization λ are labeled by the collective quantum number (37),

$$J = \{k_z, m, l\}, \qquad k_z \in \mathbb{R}, \qquad m \in \mathbb{Z}, \qquad l \in \mathbb{N}. \tag{37}$$

An integration over all three momenta $\boldsymbol{k}$ in a phase space of plane waves in an unrestricted space is reduced, in the cylinder, to the sum over the collective quantum number J:

$$\int \frac{d^3k}{(2\pi)^3} \leftrightarrow \sum_J = \frac{1}{\pi R^2} \int \frac{dk_z}{2\pi} \sum_{m\in\mathbb{Z}} \sum_{l=1}^{\infty}. \tag{38}$$

This sums appears, for example, in Eq. (17).

According to Eq. (19) the identity in the phase space of the modes with a given polarization λ is as follows:

$$\delta_{JJ'} = 2\pi^2 R^2 \delta(k_z - k'_z)\delta_{mm'}\delta_{ll'}. \tag{39}$$

An explicit calculation of the orthonormalization condition (23),

$$\int_0^R d\rho\rho f_{\mathrm{TE}}^2(\rho) = \int_0^R d\rho\rho f_{\mathrm{TM}}^2(\rho) = \frac{R^2}{2k_\perp^2}, \tag{40}$$

gives us the coefficients $C_\lambda^{\mathfrak{b}}$

$$C_{\mathrm{TE}}^E = C_{\mathrm{TM}}^M = \frac{R}{\sqrt{(\kappa'_{ml})^2 - m^2}|J_m(\kappa'_{ml})|}, \tag{41a}$$

$$C_{\mathrm{TE}}^M = C_{\mathrm{TM}}^E = \frac{R}{\kappa_{ml}|J_{m+1}(\kappa_{ml})|}, \tag{41b}$$

in the radial functions (28) of the photon polarization modes $\lambda = \mathrm{TE}$, TM obeying the $\mathfrak{b} = E$, M boundary conditions. Here we used the integral orthogonality relations of the Bessel functions (B4) and (B5), as well as the recurrence relations (B1). Notice that $\kappa'_{ml} > |m|$.

The TM and TE modes are always orthogonal to each other,

$$\int_0^R d\rho\rho \boldsymbol{\mathcal{A}}_J^{\mathrm{TE}}(\rho)\cdot\boldsymbol{\mathcal{A}}_J^{\mathrm{TM}}(\rho) \propto [m f_{\mathrm{TE}}(\rho) f_{\mathrm{TM}}(\rho)]\Big|_0^R \equiv 0, \tag{42}$$

due to the boundary conditions (31) and the fact that $mJ_m(0) \equiv 0$ for all $m \in \mathbb{Z}$.

The conserved charges of interest in this basis are the total energy and the angular momentum which are eigenvalues of the Hamiltonian and the angular momentum operators. In our normalization the normal-ordered expressions of these operators are, respectively,

$$\mathcal{H} = \int d^3x \frac{1}{2} : (\boldsymbol{E}^2 + \boldsymbol{B}^2) := \sum_{J,\lambda} \omega_J^{(\lambda)} \hat{a}_J^{(\lambda)\dagger} \hat{a}_J^{(\lambda)}, \tag{43}$$

$$L_\varphi = \int d^3x : P_\varphi := \sum_{J,\lambda} m \hat{a}_J^{(\lambda)\dagger} \hat{a}_J^{(\lambda)}. \tag{44}$$

3. Modes in an unbounded space with $R \to \infty$

As a final point in this section we will discuss the limit of an unbounded space $R \to \infty$. First let us note that without imposing any boundary conditions we have

$$\boldsymbol{\nabla} \times \boldsymbol{\mathcal{A}}_J^{(TE,TM)} = \omega \boldsymbol{\mathcal{A}}_J^{(TM,TE)}. \tag{45}$$

We can therefore introduce eigenvectors of the curl operator

$$\boldsymbol{\mathcal{A}}_J^{\pm} = \boldsymbol{\mathcal{A}}_J^{TE} \pm \boldsymbol{\mathcal{A}}_J^{TM} \tag{46}$$

with the eigenvalues

$$\boldsymbol{\nabla} \times \boldsymbol{\mathcal{A}}_J^{\pm} = \pm\omega \boldsymbol{\mathcal{A}}_J^{\pm}. \tag{47}$$

In terms of electric and magnetic fields these modes fulfill the relations

$$\boldsymbol{B}_J^{\pm} = \mp i \boldsymbol{E}_J^{\pm}, \tag{48}$$

which show that these modes correspond to left- and right-circularly polarized electromagnetic fields. The gauge potential can now be quantized in this basis as follows:

$$\boldsymbol{\mathcal{A}} = \sum_J \frac{\sqrt{2}}{\sqrt{\omega_J}} (\boldsymbol{\mathcal{A}}_J^{(+)} \alpha_J^{(+)} + \boldsymbol{\mathcal{A}}_J^{(-)*} \alpha_J^{(-)\dagger}). \tag{49}$$

Similarly to the finite-radius cases, the radial scalar functions f_λ are still proportional to the Bessel function (28). However the radial momentum $k_\perp$ is not quantized in the absence of the boundaries. The wave functions are still normalized according to the condition

$$\int d^3x \boldsymbol{\mathcal{A}}_{mk}^{(\lambda)*}(x) \boldsymbol{\mathcal{A}}_{m',k'}^{(\lambda')}(x) = \delta_{\lambda\lambda'}\delta_{JJ'} \tag{50}$$

with the collective quantum number $J = (m, k, k_\perp)$ and

$$\delta_{JJ'} = 4\pi^2 \delta_{mm'} \delta(k_z - k'_z) \frac{\delta(k_\perp - k'_\perp)}{k_\perp}, \tag{51}$$

$$\sum_J = \int_{-\infty}^{+\infty} \frac{dk_z}{2\pi} \sum_{m\in\mathbb{Z}} \int_0^\infty \frac{k_\perp dk_\perp}{2\pi}. \tag{52}$$

The normalization constant in this unbounded case is $C = \frac{1}{\sqrt{2}k_\perp}$. Since the wave functions for both circular polarizations obey the same boundary conditions (see below), the normalization constant is the same for both polarizations. The complex field $\boldsymbol{\mathcal{E}} = \boldsymbol{E} + i\boldsymbol{B}$ is then just $\boldsymbol{\mathcal{E}} = \boldsymbol{\nabla} \times \boldsymbol{\mathcal{A}}$.

Quantization is achieved by

$$[\alpha_J^{(\lambda)\dagger}, \alpha_K^{(\mu)}] = \delta_{JK} \delta^{\lambda\mu}. \tag{53}$$

The wave functions form an orthonormal system

$$\int d^3x \boldsymbol{\mathcal{A}}_K^{(\lambda)*} \cdot \boldsymbol{\mathcal{A}}_L^{(\mu)} = \delta_{K,L} \delta^{\lambda,\mu}. \tag{54}$$

We note that $\boldsymbol{E} \pm i\boldsymbol{B}$ are eigenvectors of the duality transformation $(\boldsymbol{E}, \boldsymbol{B}) \to (\boldsymbol{B}, -\boldsymbol{E})$ with eigenvalues $\pm i$. The Hamiltonian is $\mathcal{H} = \frac{1}{2} \boldsymbol{\mathcal{E}} \cdot \boldsymbol{\mathcal{E}}^\dagger$. Both polarization modes have the same frequencies. Therefore the Hamiltonian is

$$\mathcal{H} = \sum_J \omega_J (\alpha_J^{(+)\dagger} \alpha_J^{(+)} + \alpha_J^{(-)\dagger} \alpha_J^{(-)}), \tag{55}$$

with $\omega_J^2 = k_z^2 + k_\perp^2$ as in Eq. (25). The projection of the angular momentum on the z axis can be computed from the expression of the Poynting vector $\boldsymbol{P} = \frac{i}{2} \boldsymbol{\mathcal{E}} \times \boldsymbol{\mathcal{E}}^\dagger$ as

$$L_\varphi = \sum_J m (\alpha_J^{(+)\dagger} \alpha_J^{(+)} + \alpha_J^{(-)\dagger} \alpha_J^{(-)}). \tag{56}$$

C. Helicity and zilch

Back in the 1960s Lipkin found a new conserved charge for the free Maxwell theory which he called the "zilch" [25]. Soon afterwards Kibble pointed out that there are infinitely many such zilch currents [26].

The basic observation is the following: if $(\boldsymbol{E}, \boldsymbol{B})$ and $(\boldsymbol{H}, \boldsymbol{G})$ are doublets of fields obeying the free Maxwell's equations

$$\nabla \cdot \boldsymbol{E} = \nabla \cdot \boldsymbol{B} = \nabla \cdot \boldsymbol{H} = \nabla \cdot \boldsymbol{G} = 0, \tag{57}$$

$$\nabla \times \boldsymbol{B} - \frac{\partial \boldsymbol{E}}{\partial t} = \nabla \times \boldsymbol{E} + \frac{\partial \boldsymbol{B}}{\partial t} = 0, \tag{58}$$

$$\nabla \times \boldsymbol{H} - \frac{\partial \boldsymbol{G}}{\partial t} = \nabla \times \boldsymbol{G} + \frac{\partial \boldsymbol{H}}{\partial t} = 0, \tag{59}$$

then the expressions

$$\zeta = \frac{\boldsymbol{H} \cdot \boldsymbol{B} + \boldsymbol{G} \cdot \boldsymbol{E}}{2}, \tag{60}$$

$$\boldsymbol{J}_\zeta = -\frac{\boldsymbol{H} \times \boldsymbol{E} + \boldsymbol{G} \times \boldsymbol{B}}{2}, \tag{61}$$

fulfill the conservation law

$$\frac{\partial \zeta}{\partial t} + \nabla \cdot \boldsymbol{J}_\zeta = 0. \tag{62}$$

If we identify $\boldsymbol{H} \to \boldsymbol{A}$ with the vector potential and $\boldsymbol{G} \to \boldsymbol{C}$ with the dual vector potential in the Coulomb gauge $\nabla \cdot \boldsymbol{A} = \nabla \cdot \boldsymbol{C} = 0$, then

$$\boldsymbol{B} = \nabla \times \boldsymbol{A} = \frac{\partial \boldsymbol{C}}{\partial t}, \tag{63}$$

$$\boldsymbol{E} = -\frac{\partial \boldsymbol{A}}{\partial t} = \nabla \times \boldsymbol{C}. \tag{64}$$

The conserved charge (60) in this case is the optical helicity. The inconvenience with these definitions is that they do depend on the gauge choice. The vector and dual vector potential define a zilch current only in the Coulomb gauge (16)!

Lipkin's original zilch is gauge-invariant and local. It can be defined by taking

$$\boldsymbol{H} = \nabla \times \boldsymbol{B}, \tag{65}$$

$$\boldsymbol{G} = \nabla \times \boldsymbol{E}. \tag{66}$$

If one allows for nonlocal expressions one can define the k-zilch currents by taking

$$\boldsymbol{H}_s = \Delta^{-s} \boldsymbol{\nabla} \times \boldsymbol{B}, \tag{67}$$

$$\boldsymbol{G}_s = \Delta^{-s} \boldsymbol{\nabla} \times \boldsymbol{E}, \tag{68}$$

where Δ is the Laplace operator. If one uses the Coulomb gauge (16) then the 1-zilch ($s = 1$) becomes local in terms of the vector potentials $\boldsymbol{A}$, $\boldsymbol{C}$ and it coincides with the "optical helicity" given in a relativistic form in Eq. (2). The 1-zilch is also unique in the sense that it is the only one of the s-zilches that has the correct dimension of a conserved current, i.e., three. In contrast Lipkin's gauge-invariant local zilch current, the 0-zilch, has dimension five, and is often associated with "the optical chirality flow" [34,35].

For the finite-radius case, the perfect electric (12) and magnetic (14) conductor boundary conditions do not respect the zilch. The helicity (or zilch) influx

$$\begin{aligned}\boldsymbol{J}_h \cdot \boldsymbol{n} &\equiv J_{h,r}(R) \\ &= (E_\varphi A_z - E_z A_\varphi + C_\varphi B_z - C_z B_\varphi)|_{\rho=R}, \end{aligned} \tag{69}$$

does not vanish identically at the boundary.

In the helicity eigenstate basis in the unbounded domain the helicity and the zilch can be expressed by the complex fields

$$h = \frac{1}{4}(\boldsymbol{\mathcal{A}}^\dagger \cdot \boldsymbol{\mathcal{E}} + \boldsymbol{\mathcal{A}} \cdot \boldsymbol{\mathcal{E}}^\dagger), \tag{70}$$

$$\zeta = \frac{1}{4}(\boldsymbol{\mathcal{G}}^\dagger \cdot \boldsymbol{\mathcal{E}} + \boldsymbol{\mathcal{E}} \cdot \boldsymbol{\mathcal{G}}^\dagger). \tag{71}$$

The normal-ordered integrated total charges (helicities and zilches) are, respectively,

$$Q_h = \int d^3x :h: = \sum_J (\alpha_J^{(+)\dagger}\alpha_J^{(+)} - \alpha_J^{(-)\dagger}\alpha_J^{(-)}), \tag{72}$$

$$Q_\zeta = \int d^3x :\zeta: = \sum_J \omega_J^2 (\alpha_J^{(+)\dagger}\alpha_J^{(+)} - \alpha_J^{(-)\dagger}\alpha_J^{(-)}). \tag{73}$$

As expected, helicity in the Coulomb gauge counts the number of right-circularly polarized photons minus the number of left-circularly polarized photons. The gauge-invariant zilch charge weights these numbers with the squares of the frequencies and is therefore a good gauge-invariant observable and local measure of helicity [30].

The expressions of the helicity and zilch currents in terms of the complex fields are

$$\boldsymbol{J}_h = \frac{i}{4}(\boldsymbol{\mathcal{A}} \times \boldsymbol{\mathcal{E}}^\dagger - \boldsymbol{\mathcal{A}}^\dagger \times \boldsymbol{\mathcal{E}}), \tag{74}$$

$$\boldsymbol{J}_\zeta = \frac{i}{4}(\boldsymbol{\mathcal{E}} \times \boldsymbol{\mathcal{G}}^\dagger - \boldsymbol{\mathcal{E}}^\dagger \times \boldsymbol{\mathcal{G}}). \tag{75}$$

D. Unbounded domain

We will now study the problem of the generation of the helicity and zilch currents at the center of rotation in an unbounded domain. The analogous problem for chiral fermions is known to give a well-defined expression that coincides to lowest order in the angular momentum with the predictions from anomaly-induced transport theory—the chiral vortical effect. It also predicts terms of higher order in Ω but their status is somewhat less clear. We will follow the strategy that worked for chiral fermions as closely as possible.

The thermal expectation value of the helicity current in the unbounded domain is formally

$$\begin{aligned}\langle J_h^z(\rho)\rangle_{T,\Omega}^\infty &= \int_{\Omega^+}^\infty \frac{dk_\perp}{2\pi}\int_{-\infty}^\infty \frac{dk}{2\pi}\sum_m n_B(\omega - m\Omega, T) \\ &\quad\times 2m\left(1+\frac{k^2}{\omega^2}\right)\frac{J_m(k_\perp\rho)J_m'(k_\perp\rho)}{\rho}. \end{aligned} \tag{76}$$

where $n_B(\varepsilon, T) = [\exp(\varepsilon/T) - 1]^{-1}$ is the occupation number and the eigenenergy ω is given in Eq. (25). Both photon polarizations contribute the same amount to the current (76). Since the current (76) should be understood as the limit $R \to \infty$ of the finite-radius theory there is in principle a lower limit on the $k_\perp$ integration. At any finite radius we have $\Omega R < 1$ and $k_\perp = \frac{\kappa_{ml}}{R}$ with $\kappa_{ml} > m$. Therefore we always have $k_\perp > \Omega$ in Eq. (76).

One observation is that the total current also vanishes in the unbounded domain. Indeed we integrate the current (76) over the (infinite) cross section of the cylinder as in Eq. (104) and then use the identity (100) to show that the contribution of every eigenmode $f_J(\rho) = J_m(k_\perp\rho)$ is proportional to $J_m^2(k_\perp R)$ which vanishes in the infinite-volume limit $R \to \infty$.

If we concentrate on the other hand on the center of rotation $\rho = 0$ we find that only the modes with $m = \pm 1$ contribute. We can also change the integration variable from $k_\perp$ to ω to find

$$\begin{aligned}\langle J_h^z(0)\rangle_{T,\Omega}^\infty &= \frac{1}{8\pi^2}\int_{\Omega^+}^\infty d\omega \int_{-\omega}^\omega dk\left(\omega + \frac{k^2}{\omega}\right) \\ &\quad\times\left[\frac{1}{e^{(\omega-\Omega)/T}-1} - \frac{1}{e^{(\omega+\Omega)/T}-1}\right]. \end{aligned} \tag{77}$$

We can now expand the integral to lowest order in powers of Ω/T and find

$$\langle J_h^z(0)\rangle_{T,\Omega}^\infty = \frac{4T^2\Omega}{3\pi^2}\int_0^\infty dx\frac{x}{e^x - 1} = \frac{2T^2}{9}\Omega. \tag{78}$$

One can also try to proceed by ignoring the lower bound on the integration over the frequency ω in the first integral in Eq. (77). This leads to

$$\begin{aligned}\langle J_h^z(0)\rangle_{T,\Omega}^{\infty,(\mathrm{formal})} &= \frac{T^3}{3\pi^2}\int_0^\infty dx x^2 \\ &\quad\times\left[\frac{1}{e^{x-\Omega/T}-1} - \frac{1}{e^{x+\Omega/T}-1}\right]. \end{aligned} \tag{79}$$

In order to evaluate this we can use the integral representation of the polylogarithms together with the Jonquière inversion relation

$$Li_n(z) = \frac{1}{\Gamma(n)} \int_0^\infty \frac{t^{n-1}}{e^t/z - 1},$$
$$Li_n(z) + (-1)^n Li_n(1/z) = -\frac{(2\pi i)^2}{n!} B_n\left(\frac{1}{2} \pm \frac{\ln(-z)}{2\pi i}\right).$$

Here $B_n(x)$ is the nth Bernoulli polynomial and the sign is chosen according to $z \notin [0,1]$ or $z \notin]1,\infty]$. This leads to the following formal expression:

$$\langle J_h^z(0)\rangle_{T,\Omega}^{\infty,(\mathrm{formal})} = \frac{2T^2}{9}\Omega \pm i\frac{T}{3\pi}\Omega^2 - \frac{1}{9\pi^2}\Omega^3, \tag{80}$$

which is clearly unphysical beyond the leading order in the angular momentum Ω. The reason is that the integrand in Eq. (77) always has at least one pole at frequency $\omega = |\Omega|$. The analogous integrals for fermions are well defined since the Fermi-Dirac distribution does not present a singularity. However even in the fermionic case the higher-order terms do not seem to be universal [7].

The same considerations hold for the zilch current as well. The only difference is an additional insertion of ω^2 under the integral in Eq. (76). We only quote the infinite-volume result for the on-axis zilch current obtained to linear order in Ω:

$$\langle J_\zeta^z(0)\rangle_{T,\Omega}^{\infty} = \frac{8\pi^2 T^4}{45}\Omega. \tag{81}$$

III. Rotations

We will study the rotating ensemble in a vacuum defined with respect to a fixed laboratory frame. In this case rotation is implemented by defining the statistical operator

$$\rho = \frac{1}{Z} e^{-\beta(\mathcal{H} - \Omega L_\varphi)}, \tag{82}$$

where $\beta = 1/T$ is the inverse temperature, Ω is the angular frequency corresponding to a uniform rotation with angular velocity $\boldsymbol{\Omega} = \Omega \mathbf{e}_z$ about the z axis, $\mathcal{H}$ is the Hamiltonian (55) and L_φ is the projection of the angular momentum operator on the rotation axis (56). Without losing generality we assume that the cylinder rotates counterclockwise with $\Omega \geq 0$.

Rotating ensembles of relativistic field theories are notoriously ill-defined whenever the tangential velocity at radius ρ exceeds the speed of light. A well-defined ensemble is therefore possible only as long as $R\Omega < 1$, where the speed of light $c = 1$ in our conventions. This makes it immediately clear that the unbounded domain with a constant angular velocity does not give rise to a consistent statistical ensemble. As noted however long ago by Vilenkin, in the case of fermions it is possible to extract meaningful results for the statistical average of the current at the center of rotation. As we will discuss in detail, for photons even this property is not realized beyond the lowest order in Ω.

In principle one can study the ensemble both in a corotating and in a laboratory (nonrotating) frame and define two different vacua. A nonrotating vacuum has been considered by Vilenkin [12] while the rotating vacuum has been studied by Iyer [36]. One may show that both approaches are equivalent provided the system is bounded in such a way that the velocity of the rigidly rotating body does not exceed the speed of light so that causality is respected. Technically, the nonrotating (Vilenkin) vacuum is equivalent to the rotating (Iyer) vacuum if the energy of each eigenmode in the laboratory frame ε and in the corotating frame $\tilde{\varepsilon}$ satisfy the relation $\varepsilon\tilde{\varepsilon} > 0$. This relation always holds when causality is respected. Causality is violated in a rigidly rotating unbounded space, in which $\varepsilon\tilde{\varepsilon} < 0$ for certain modes and, consequently, the nonrotating and rotating vacua are not equivalent [13]. The unbounded rotating systems may have several pathologies related to instabilities and the rotation-induced Unruh effect [37,38]. Further discussions, in particular on the difference between fermionic and bosonic states, may be found in Ref. [13].

The thermal expectation value of an operator $\mathcal{O}$ for a uniformly rotating ensemble is

$$\langle\hat{\mathcal{O}}(x)\rangle_{T,\Omega} = \sum_{J,\lambda} n_B(T,\Omega;J,\lambda)\langle\hat{\mathcal{O}}(x)\rangle_J, \tag{83}$$

where $\langle\hat{\mathcal{O}}(x)\rangle_J \equiv \langle J|\mathcal{O}|J\rangle$ corresponds to the value of the operator $\mathcal{O}$ for a photon in the state characterized by the polarization λ and the kinetic quantum numbers J (37), and

$$n_B(T,\Omega;J,\lambda) = \frac{1}{e^{(\omega_J^{(\lambda)} - m\Omega)/T} - 1} \tag{84}$$

is the Bose-Einstein distribution function at nonzero temperature T and angular velocity Ω.

In order to calculate the expectation values of the normal-ordered operators of interest we collect the mode expansions of the different fields

$$\boldsymbol{A} = \sum_{J,\lambda} \frac{1}{\sqrt{2\omega_J^{(\lambda)}}} (\boldsymbol{\mathcal{A}}_J^{(\lambda)} \hat{a}_J^{(\lambda)} + \boldsymbol{\mathcal{A}}_J^{(\lambda),*} \hat{a}_J^{(\lambda)\dagger}), \tag{85}$$

$$\boldsymbol{C} = \sum_{J,\lambda} \frac{i}{\sqrt{2\omega_J^{(\lambda)}}} (\tilde{\boldsymbol{\mathcal{A}}}_J^{(\lambda)} \hat{a}_J^{(\lambda)} - \tilde{\boldsymbol{\mathcal{A}}}_J^{(\lambda),*} \hat{a}_J^{(\lambda)\dagger}), \tag{86}$$

$$\boldsymbol{E} = \sum_{J,\lambda} \frac{i\sqrt{\omega_J^{(\lambda)}}}{\sqrt{2}} (\boldsymbol{\mathcal{A}}_J^{(\lambda)} \hat{a}_J^{(\lambda)} - \boldsymbol{\mathcal{A}}_J^{(\lambda),*} \hat{a}_J^{(\lambda)\dagger}), \tag{87}$$

$$\boldsymbol{B} = \sum_{J,\lambda} \frac{\sqrt{\omega_J^{(\lambda)}}}{\sqrt{2}} (\tilde{\boldsymbol{\mathcal{A}}}_J^{(\lambda)} \hat{a}_J^{(\lambda)} + \tilde{\boldsymbol{\mathcal{A}}}_J^{(\lambda),*} \hat{a}_J^{(\lambda)\dagger}), \tag{88}$$

$$\boldsymbol{H} = \sum_{J,\lambda} \frac{(\omega_J^{(\lambda)})^{3/2}}{\sqrt{2}} (\boldsymbol{\mathcal{A}}_J^{(\lambda)} \hat{a}_J^{(\lambda)} - \boldsymbol{\mathcal{A}}_J^{(\lambda),*} \hat{a}_J^{(\lambda)\dagger}), \quad (89)$$

$$\boldsymbol{G} = \sum_{J,\lambda} \frac{i(\omega_J^{(\lambda)})^{3/2}}{\sqrt{2}} (\tilde{\boldsymbol{\mathcal{A}}}_J^{(\lambda)} \hat{a}_J^{(\lambda)} + \tilde{\boldsymbol{\mathcal{A}}}_J^{(\lambda),*} \hat{a}_J^{(\lambda)\dagger}), \quad (90)$$

where the dual wave functions $\tilde{\boldsymbol{\mathcal{A}}}$ are defined via the relation $\nabla \times \boldsymbol{\mathcal{A}}_J^{(\lambda)} = \omega \tilde{\boldsymbol{\mathcal{A}}}_J^{(\lambda)}$.

Now we can compute the thermal averages of the following normal-ordered operators:

$$\text{optical helicity:}\ J_h^0 = \frac{1}{2} :(\boldsymbol{A} \cdot \boldsymbol{B} + \boldsymbol{C} \cdot \boldsymbol{E}):, \quad (91)$$

$$\boldsymbol{J}_h = \frac{1}{2} :(\boldsymbol{E} \times \boldsymbol{A} + \boldsymbol{C} \times \boldsymbol{B}):, \quad (92)$$

$$\text{zilch:}\ J_\zeta^0 = \frac{1}{2} :(\boldsymbol{H} \cdot \boldsymbol{B} + \boldsymbol{G} \cdot \boldsymbol{E}):, \quad (93)$$

$$\boldsymbol{J}_\zeta = \frac{1}{2} :(\boldsymbol{E} \times \boldsymbol{H} + \boldsymbol{G} \times \boldsymbol{B}):, \quad (94)$$

$$\text{Poynting vector:}\ \boldsymbol{J}_\epsilon =:\boldsymbol{E} \times \boldsymbol{B}:. \quad (95)$$

We note that all of these expressions are duality invariant: $(\boldsymbol{E},\boldsymbol{B}) \to (-\boldsymbol{B},\boldsymbol{E})$, $(\boldsymbol{C},\boldsymbol{A}) \to (-\boldsymbol{A},\boldsymbol{C})$ etc. They are normal ordered (with creation operators placed on the left) and we only need the one-particle expectation values to evaluate the thermal averages.

It is worth mentioning that we quantize the gauge field A_μ in the Coulomb gauge (16) formulated in the laboratory frame. This gauge condition is not satisfied by the fields in the corotating frame A'_μ which are related to the ones in the laboratory frame by the linear transformation $\boldsymbol{A}' = \boldsymbol{A}$ and $A'_0 = A_0 - \Omega\rho A_\varphi$. The spatial part of the Coulomb gauge is thus respected by the corotating gauge fields, $\boldsymbol{\nabla}' \cdot \boldsymbol{A}' = 0$, while the temporal component of the gauge field in the corotating frame is nonzero, $A'_0 \neq 0$, for both TE and TM photon polarizations (26). However, since all observables of interest are formulated in the laboratory frame, and the vacua for both the laboratory and rotating frames are the same, the quantization should be done in the Coulomb gauge (16) with respect to the gauge fields in the laboratory frame. Moreover, the uniform rotation affects the expectation values of the observables in the laboratory frame via the Bose-Einstein distribution function (84), which depends on the photon energy spectrum in the corotating frame, $\omega'_J = \omega_J - m\Omega$. Since the latter is a gauge-independent quantity, the choice of the gauge in the corotating frame has no effect on the expectation values of the observables.

The optical helicity, zilch and their currents have the single-particle expectation values

$$\langle J|J^0_{h,\zeta}|J\rangle = 2km(\omega_J)^{1-2s} \frac{f_J f'_J}{\rho}, \quad (96)$$

$$\langle J|\boldsymbol{J}_{h,\zeta}|J\rangle = \begin{pmatrix} 0 \\ kk_\perp^2(\omega_J)^{-2s} f_J f'_J \\ m(\omega_J)^{2-2s}(1+\frac{k^2}{\omega_J^2})\frac{f_J f'_J}{\rho} \end{pmatrix} \quad (97)$$

where $s=1$ for the optical helicity and $s=0$ for the zilch. We note that these quantities fulfill the Ward identity

$$\omega\langle J|J^0_{h,\zeta}|J\rangle - \frac{m}{\rho}\langle J|J^\varphi_{h,\zeta}|J\rangle - k\langle J|J^z_{h,\zeta}|J\rangle = 0, \quad (98)$$

associated with the zilch conservation (62) and with a similar conservation relation for the helicity.

The expectation value of the Poynting vector is

$$\langle J|\vec{J}_\epsilon|J\rangle = \begin{pmatrix} 0 \\ \frac{m}{\rho} k_\perp^2 f_J^2 \\ k(\frac{m^2}{\rho^2} f_J^2 + f'^2_J) \end{pmatrix}. \quad (99)$$

For simplicity of notation we have suppressed the polarization index in the above. The expressions are formally the same for both polarizations.

Since the energy ω_J is an even function of the momentum in the z direction, k_z, all thermal expectation values of expressions linear in k_z vanish upon integration. The linearity in k_z immediately tells us that $h = \zeta = J^z_\epsilon = J^\varphi_h = J^\varphi_\zeta = 0$ in addition to the obvious absence of the radial currents $J^\rho_\epsilon = J^\rho_h = J^\rho_\zeta = 0$.

Furthermore, from the identity

$$2m\int_0^R \rho d\rho \frac{ff'}{\rho} = mf(R)^2, \quad (100)$$

it follows that only those modes that obey the Neumann boundary conditions on the radial photon functions f_J give us a nonzero net helicity and zilch currents! The correspondence between the boundary conditions on the radial photon functions, the photon polarizations and the type of boundary conditions can be found in Eq. (31).

In the general case, the thermal expectation values cannot be evaluated analytically and therefore we proceed to their numerical evaluation. For the numerical summation it is convenient to write the energy and angular momentum densities as follows:

$$R^4\epsilon = \frac{1}{\pi^2}\sum_{m,l,\lambda}\int_0^\infty dq \frac{\nu_J^{(\lambda)}}{e^{\frac{\nu_J^{(\lambda)} - mR\Omega}{RT}} - 1}, \quad (101)$$

$$R^3 L_\varphi = \frac{1}{\pi^2}\sum_{m,l,\lambda}\int_0^\infty dq \frac{m}{e^{\frac{\nu_J^{(\lambda)} - mR\Omega}{RT}} - 1}. \quad (102)$$

In order to adapt these quantities for a numerical evaluation we used a shorthand notation $\nu_J^{(\lambda)} \equiv R\omega_J^{(\lambda)}$ for the dimensionless energy, characterized by the cumulative index J of

Eq. (37) and by the polarization $\lambda = \mathrm{TE}/\mathrm{TM}$ according to the type of boundary condition (36).

In Fig. 1 we show the appropriately normalized energy (101), angular momentum (102) and moment of inertia

$$I(\Omega, T) = \frac{L_\varphi(\Omega, T)}{\Omega}, \tag{103}$$

as functions of the angular frequency Ω for various fixed temperatures T.

The components of the total helicity and zilch currents along the axis of rotation, given by integration over local currents (97) over the cross section of the cylinder,

$$J_s^{z,\mathrm{tot}} = \int_0^R \rho d\rho \int_0^{2\pi} d\varphi J_s(\rho, \varphi), \tag{104}$$

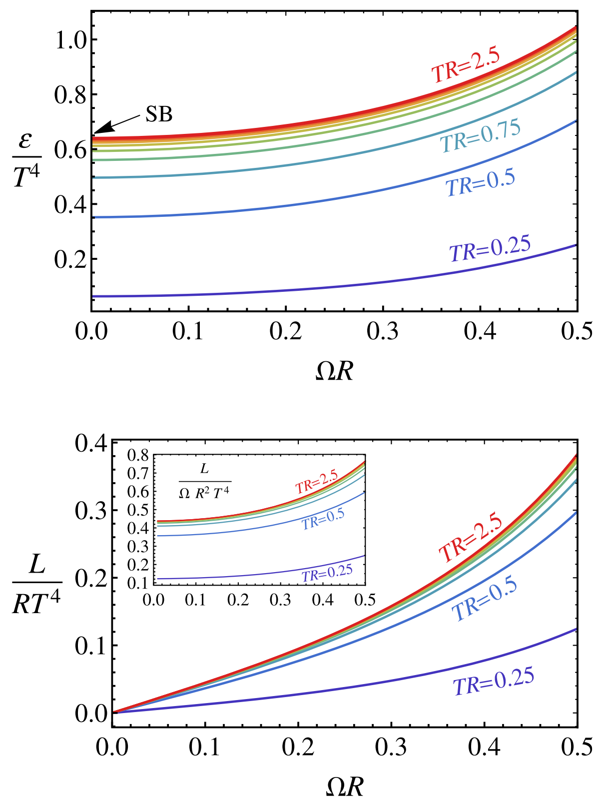

FIG. 1. The energy (101) and angular momentum (102) densities as functions of the dimensionless tangential velocity at the boundary $R\Omega$. We restrict ourselves to relatively low angular velocities $R\Omega < 0.5$ to facilitate numerical evaluation. The plots show that the behavior of the dimensionless quantities ϵ/T^4 (top) and $L/(RT^3)$ (bottom) for a temperature range from $TR = 0.25$ up to $TR = 2.5$ in steps of $\delta(TR) = 0.25$. As it can be seen from the plots, both of these dimensionless quantities collapse on a universal high-temperature curve. The arrow in the upper plot marks the Stefan-Boltzmann value $\epsilon = \frac{T^4\pi^2}{15}$. At temperature $TR = 2.5$ the system is already within 3% of this value at zero rotation. The inset in the lower figure shows the moment of inertia (103) with the corresponding Stefan-Boltzmann value.

are as follows:

$$J_s^{z,\mathrm{tot}} R^{2-2s} = \frac{1}{\pi} \sum_{m,l} \int_0^\infty dq \frac{1 + \frac{q^2}{(\nu_J^{(\lambda)})^2}}{(\kappa'_{ml})^2 - m^2} \frac{m(\nu_J^{(\lambda)})^{2-2s}}{e^{\frac{\nu_J^{(\lambda)} - mR\Omega}{RT}} - 1}, \tag{105}$$

where $s = 1$ corresponds to the helicity and $s = 0$ to the zilch currents (also denoted, respectively, as $s = h$ and $s = \zeta$ below). In Eq. (105) we chose the polarization λ taking into account the fact [Eq. (100)] that only the modes with the Neumann boundary conditions on the radial photon functions $f_J(\rho)$ may contribute.

In Fig. 2 we show the total helicity and zilch currents (105) which are increasing functions of both temperature and angular momentum. Its important to remember that the total currents, contrary to the infinite-volume expression, are nonvanishing only because of the Neumann boundary condition imposed on radial photon functions. The net flux of helicity and zilch is therefore interpreted as an effect of the duality-breaking boundary conditions. Qualitatively both quantities exhibit increasing flux with increasing angular velocity.

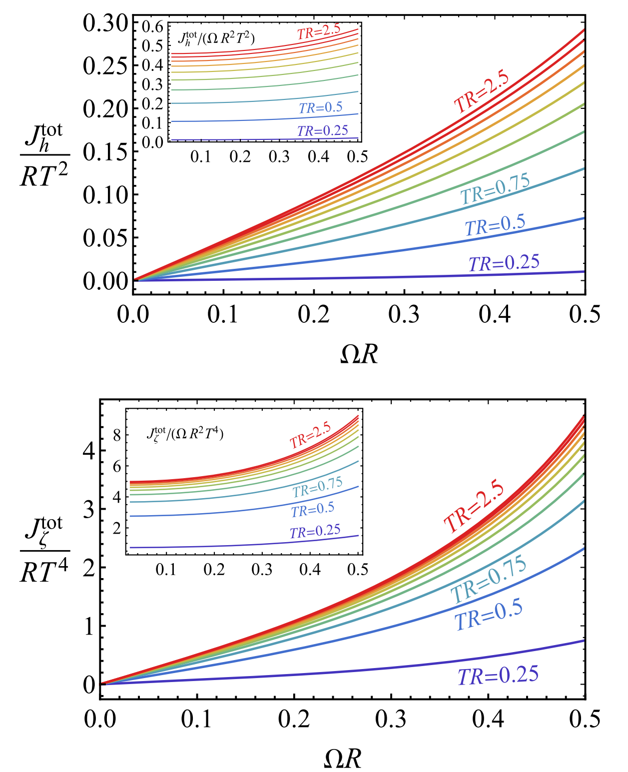

FIG. 2. The total helicity ($s = 1$) and zilch ($s = 0$) currents (105) as functions of the dimensionless tangential velocity at the boundary $R\Omega$. The plots show the behavior of the dimensionless quantities $J_h^{z,\mathrm{tot}}/(RT^2)$ and $J_\zeta^{z,\mathrm{tot}}/(RT^4)$ for the same temperature range as in Fig. 1. The insets show the currents divided by the frequency Ω.

It is well seen in Fig. 2 that in the limit of small angular frequencies, $\Omega \to 0$, both the total helicity and the total zilch currents (105) exhibit a linear dependence on Ω:

$$J_s^{z,\mathrm{tot}} = C_s(T) T^{4-2s} \Omega + O(\Omega^2). \tag{106}$$

In Fig. 3 we show the dimensionless coefficients C_s as functions of temperature T. Both quantities vanish exponentially in the limit of small temperatures $T \to 0$, while in the limit of high temperature they approach the values

$$C_h(T \to \infty) \approx 0.65, \qquad C_\zeta(T \to \infty) \approx 5.42, \tag{107}$$

respectively.

Finally using the series expansion of the Bessel functions, $J_m(x) = (x/2)^m + O(x^{m+2})$, it follows that the helicity and zilch current densities at the axes of rotation $\rho = 0$ receive only contributions from the angular momenta $m = \pm 1$:

$$J_s^z(0) R^{2-2s} = \frac{1}{\pi^2} \sum_{l,\lambda} \int_0^\infty dq (\nu_J^{(\lambda)})^{(2-2s)} \left(1 + \frac{q^2}{(\nu_J^{(\lambda)})^2}\right) \cdot C_\lambda^2 \left(\frac{\kappa_{1,l}^\lambda}{2R}\right)^2 \left[\frac{1}{e^{\frac{\nu_J^{(\lambda)} - R\Omega}{RT}} - 1} - \frac{1}{e^{\frac{\nu_J^{(\lambda)} + R\Omega}{RT}} - 1}\right], \tag{108}$$

where again $s = 1$ and $s = 0$ correspond to the helicity and the zilch, respectively. The $m = \pm 1$ eigen-numbers $\kappa_{1,l}^\lambda \equiv \kappa_{-1,l}^\lambda$ for both polarizations $\lambda = \mathrm{TE}/\mathrm{TM}$ can be read off from Eqs. (34) and (35), and the normalization coefficients C_λ are given in Eq. (41).

The helicity and zilch currents (108) at the axis of rotation $\rho = 0$ are shown in Fig. 4 as functions of temperature T. We plot these currents in the limit of slow rotations $\Omega \to 0$ and normalize them to the corresponding results obtained in the unbounded domain (78) and (81), to be discussed in the next section. The high-temperature limit approaches the value of the linear truncation in Ω in the unbounded domain. Its interesting that this convergence is faster for the zilch current than for the helicity current. The insets show the exponential onset of the currents for small temperatures.

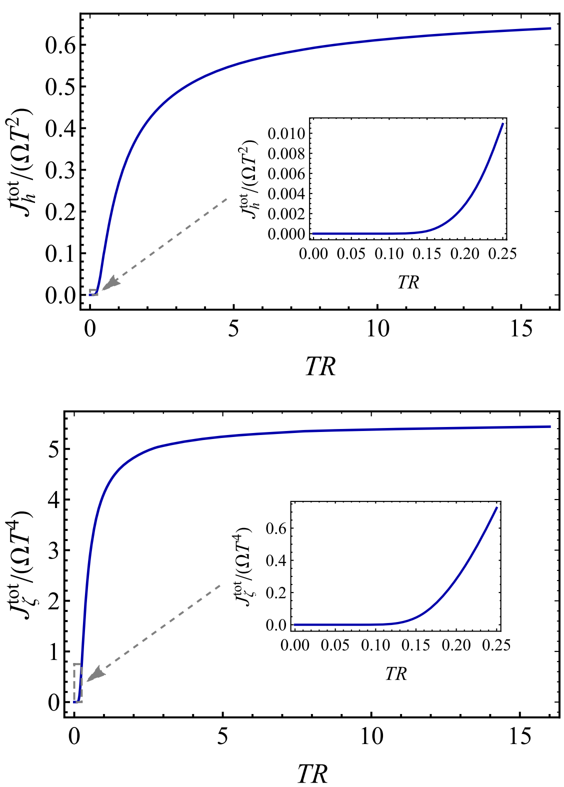

FIG. 3. The dimensionless strengths of the helicity ($s = 1$) and zilch ($s = 0$) currents (106) in the limit of small angular frequencies $\Omega \to 0$ as functions of temperature T. The insets show the exponential onset of both currents at small temperatures.

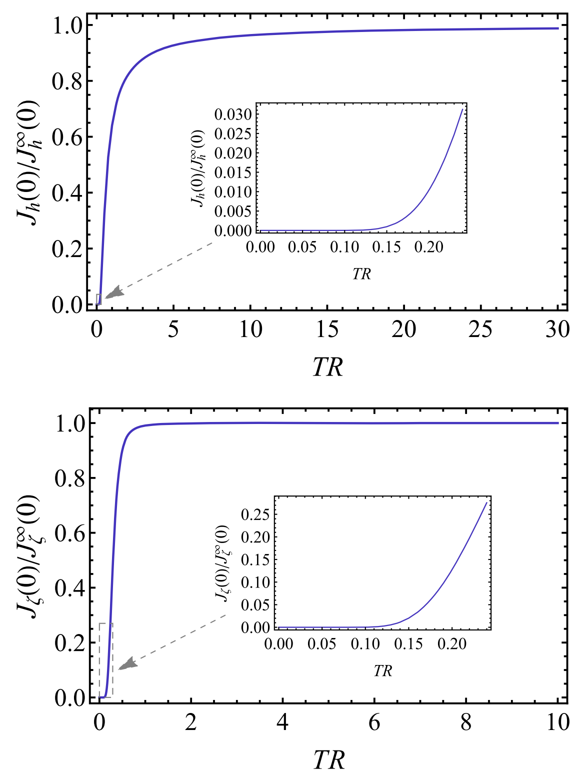

FIG. 4. Values of the helicity ($s = 1$) and zilch ($s = 0$) current densities (108) at the axes of rotation $\rho = 0$ for very low angular velocities. The results are plotted as functions of TR and as fractions of the result in the unbounded domain (78) and (81) respectively. The insets show the currents at small temperatures.

IV. DISCUSSION AND CONCLUSION

We have studied helicity and zilch photonic currents in the free Maxwell theory induced by rotation in a bounded cylindrical domain. An important role is played by the conditions imposed on photons at the boundary of the cylinder. We have chosen two types of boundary conditions corresponding to perfect electric and perfect magnetic conductors as both of these conditions guarantee that the influx of energy and angular momentum vanishes at the boundary. The values of the helicity and zilch photonic currents for both types of boundaries are the same because these boundary conditions are exchanged under a discrete electric-magnetic duality transformation while all expressions of interest are duality invariant.

In searching for an analogue of the well-known CVE of chiral fermions we studied the current densities at the axis of rotation. A universal value can reasonably be expected to arise only in the high-temperature limit in which the boundary conditions play no role for the physics of photons at the center of rotation. Indeed we found that in the high-temperature limit the result for small angular velocity converges to the result obtained to linear order in Ω in the unbounded domain. However, a direct calculation in the unbounded domain is plagued with the difficulty that the integrals over the Bose-Einstein distributions are well defined only for sufficiently small angular velocities, $\Omega < 1/R$. This fact means that the angular velocity has to go to zero faster than $1/R$. Consequently, the formal result for the helicity current at the axis of rotation, obtained in the unbounded domain (80), does not seem to be physically meaningful as this procedure gives a complex value for the expectation value of a Hermitian operator.

On the contrary, a truncation of the expression for the current to lowest order in Ω in an unbounded domain provides us with the still meaningful physical result (78) because it exactly corresponds to a value to which the central current densities converge in the high-temperature limit in the bounded domain. In this sense (the leading-order truncation of the high-temperature limit) one can indeed speak of a chiral vortical effect for photons in an unbounded domain.

It is worth comparing our numerical result for the central helicity current (78) to the existing derivations of the photonic CVE in the literature [19–21]. We note that the authors of Refs. [19,21] considered the magnetic helicity current [with the results, in our notation, $J_h^z = T^2\Omega/6$ and $J_h^z = (\epsilon\mu - 1)T^2\Omega/12$, respectively] and only the authors of Ref. [20] studied a semiclassical evaluation of the optical helicity current (which gives $J_h^z = T^2\Omega/3$). Notice that the factor of 2 difference in the expressions for the helicity currents in Refs. [19,20] comes from the different definitions used for the currents, while they both differ from the helicity current of Ref. [21] which is zero in vacuum $\epsilon = \mu = 1$. In any case, our value for the helicity current (78) differs from the results obtained in all of these works.

The disagreement with the literature is probably not surprising since the helicity current is not a gauge-invariant quantity and, therefore, it cannot be considered a good physical observable. On the other hand Lipkin's zilch current is a local and gauge-invariant quantity. The zilch current at the axis of the rotating cylinder in the high-temperature limit is given in Eq. (81). It would be interesting to evaluate the expectation value of the central zilch current via Kubo formulas or in a semiclassical treatment to compare to our result (81).

Summarizing, we have found the zilch vortical effect (ZVE) which generates the helicity and zilch currents along the axis of rotation of a hot gas of photons. We have calculated these currents in a wide domain of temperatures and angular frequencies (Figs. 2 and 4) in a causality-preserving setup. For a photon gas in a fixed-size cavity, the currents vanish exponentially in the limit of low temperature. At high temperature and low angular frequency of rotation, the currents at the axis of rotation are given by Eqs. (78) and (81) while the total currents are estimated in Eqs. (106) and (107).

Both the helicity and zilch currents show qualitatively similar behavior. They constitute a part of an infinite tower of conserved charges (zilches) of free electromagnetic field. Thus, in a general sense, the ZVE is responsible for an infinite tower of anomalous transport effects in a rotating photon gas.

ACKNOWLEDGMENTS

K. L. would like to thank the participants of the workshop "Open Problems and Opportunities in Chiral Fluids," Santa Fe, especially M. Stone and A. Sadofyev for interesting and useful discussions. M. C. is grateful to D. E. Kharzeev for useful discussions. We also thank M. Elbistan and N. Yamamoto for correspondence and comments on the manuscript. This work has been supported by the PIC2016FR6/PICS07480, FPA2015-65480-P (Ministry of Economy and Competitiveness/European Regional Development Fund) and Severo Ochoa Excellence Program Grant No. SEV-2016-0597. The work of M. C. was partially supported within the state assignment of the Ministry of Science and Education of Russia (Grant No. 3.6261.2017/8.9). A. C. acknowledges financial support through the Ministry of Economy and Competitiveness/State Research Agency/European Regional Development Fund, UE Grant No. FIS2015-73454-JIN.

APPENDIX A: CYLINDRICAL COORDINATES

In cylindrical coordinates a vector

$$\mathbf{a} = a_\rho \mathbf{e}_\rho + a_\varphi \mathbf{e}_\varphi + a_z \mathbf{e}_z, \tag{A1}$$

is represented via the orthonormalized basis vectors of the cylindrical system

$$\mathbf{e}_\rho = \begin{pmatrix} \cos\varphi \\ \sin\varphi \\ 0 \end{pmatrix}, \qquad \mathbf{e}_\varphi = \begin{pmatrix} -\sin\varphi \\ \cos\varphi \\ 0 \end{pmatrix}, \qquad \mathbf{e}_z = \begin{pmatrix} 0 \\ 0 \\ 1 \end{pmatrix}, \tag{A2}$$

where φ is the azimuthal angle in the (x, y) plane, and is related to the Cartesian coordinates as follows:

$$x = \rho\cos\varphi, \qquad y = \rho\sin\varphi. \tag{A3}$$

The basic operations of the vector calculus are as follows.

The scalar product:

$$\boldsymbol{a}\cdot\boldsymbol{b} = a_\rho b_\rho + a_\varphi b_\varphi + a_z b_z. \tag{A4}$$

The vector product:

$$(\boldsymbol{a}\times\boldsymbol{b})_\rho = (a_\varphi b_z - b_\varphi a_z), \tag{A5}$$

$$(\boldsymbol{a}\times\boldsymbol{b})_\varphi = (a_z b_\rho - b_z a_\rho), \tag{A6}$$

$$(\boldsymbol{a}\times\boldsymbol{b})_z = (a_\rho b_\varphi - b_\rho a_\varphi). \tag{A7}$$

The curl (rotor) operation:

$$(\boldsymbol{\nabla}\times a)_\rho = \frac{1}{\rho}\frac{\partial a_z}{\partial\varphi} - \frac{\partial a_\varphi}{\partial z}, \tag{A8}$$

$$(\boldsymbol{\nabla}\times a)_\varphi = \frac{\partial a_\rho}{\partial z} - \frac{\partial a_z}{\partial\rho}, \tag{A9}$$

$$(\boldsymbol{\nabla}\times a)_z = \frac{1}{\rho}\frac{\partial(\rho a_\varphi)}{\partial\rho} - \frac{1}{\rho}\frac{\partial a_\rho}{\partial\varphi}. \tag{A10}$$

The divergence:

$$\boldsymbol{\nabla}\cdot\boldsymbol{a} = \frac{1}{\rho}\frac{\partial(\rho a_\rho)}{\partial\rho} + \frac{1}{\rho}\frac{\partial a_\varphi}{\partial\varphi} + \frac{\partial a_z}{\partial z}. \tag{A11}$$

The gradient:

$$\boldsymbol{\nabla}f = \frac{\partial f}{\partial\rho}\mathbf{e}_\rho + \frac{1}{\rho}\frac{\partial f}{\partial\varphi}\mathbf{e}_\varphi + \frac{\partial f}{\partial z}\mathbf{e}_z. \tag{A12}$$

The Laplacian:

$$\Delta f = \frac{1}{\rho}\frac{\partial}{\partial\rho}\left(\rho\frac{\partial f}{\partial\rho}\right) + \frac{1}{\rho^2}\frac{\partial^2 f}{\partial\varphi^2} + \frac{\partial^2 f}{\partial z^2}. \tag{A13}$$

APPENDIX B: SOME PROPERTIES OF BESSEL FUNCTIONS

The Bessel functions satisfy the following recurrence relations:

$$J_{m-1}(x) + J_{m+1}(x) = \frac{2m}{x}J_m(x), \tag{B1a}$$

$$J_{m-1}(x) - J_{m+1}(x) = 2J'_m(x). \tag{B1b}$$

For arbitrary parameters a and b one gets

$$\int_0^1 dxxJ_m(ax)J_m(bx) = \frac{bJ_m(a)J_{m-1}(b) - aJ_m(b)J_{m-1}(a)}{a^2 - b^2}, \tag{B2}$$

$$\int_0^1 dxx^2 J_m(ax)J'_m(ax) = \frac{1}{2a}J_{m-1}(a)J_{m+1}(a). \tag{B3}$$

If $a = \kappa_{ml}$ and $b = \kappa_{ml'}$ are zeros of the Bessel function, $J_m(\kappa_{ml}) = J_m(\kappa_{ml'}) = 0$, then

$$\int_0^1 dxxJ_m(\kappa_{ml}x)J_m(\kappa_{ml'}x) = \frac{\delta_{ll'}}{2}J^2_{m+1}(\kappa_{ml}). \tag{B4}$$

If $a = \kappa'_{ml}$ and $b = \kappa'_{ml'}$ are zeros of a derivative of the Bessel function, $J'_m(\kappa'_{ml}) = J'_m(\kappa'_{ml'}) = 0$, then

$$\int_0^1 dxxJ_m(\kappa'_{ml}x)J_m(\kappa'_{ml'}x) = \frac{\delta_{ll'}}{2}[J^2_m(\kappa'_{ml}) - J^2_{m+1}(\kappa'_{ml})]. \tag{B5}$$

For real positive k and k' one gets

$$\int_0^\infty d\rho\rho\left[\frac{m^2}{\rho^2}J_m(k\rho)J_m(k'\rho) + kk'J'_m(k\rho)J'_m(k'\rho)\right] \equiv k^2\int_0^\infty d\rho\rho J_m(k\rho)J_m(k'\rho) = k\delta(k-k'). \tag{B6}$$

Finally we note that for large index the asymptotic expansions of the zeros are

$$\kappa_{m1} = m + 1.8558m^{1/3} + O(m^{-2/3}), \tag{B7}$$

$$\kappa'_{m1} \sim m + 0.8086m^{1/3} + O(m^{-2/3}). \tag{B8}$$

This makes the divergence of the thermodynamic partition function for $\Omega R > 1$ explicit.

[1] D. E. Kharzeev, The chiral magnetic effect and anomaly-induced transport, Prog. Part. Nucl. Phys. **75**, 133 (2014).
[2] K. Landsteiner, Notes on anomaly induced transport, Acta Phys. Pol. B **47**, 2617 (2016).
[3] K. Landsteiner, E. Megias, and F. Pena-Benitez, Gravitational Anomaly and Transport, Phys. Rev. Lett. **107**, 021601 (2011).
[4] K. Landsteiner, E. Megias, L. Melgar, and F. Pena-Benitez, Holographic gravitational anomaly and chiral vortical effect, J. High Energy Phys. 09 (2011) 121.
[5] K. Jensen, R. Loganayagam, and A. Yarom, Thermodynamics, gravitational anomalies and cones, J. High Energy Phys. 02 (2013) 088.
[6] K. Jensen, R. Loganayagam, and A. Yarom, Chern-Simons terms from thermal circles and anomalies, J. High Energy Phys. 05 (2014) 110.
[7] M. Stone and J. Y. Kim, Mixed anomalies: Chiral vortical effect and the Sommerfeld expansion, Phys. Rev. D **98**, 025012 (2018).
[8] S. Golkar and S. Sethi, Global anomalies and effective field theory, J. High Energy Phys. 05 (2016) 105.
[9] S. D. Chowdhury and J. R. David, Anomalous transport at weak coupling, J. High Energy Phys. 11 (2015) 048.
[10] S. D. Chowdhury and J. R. David, Global gravitational anomalies and transport, J. High Energy Phys. 12 (2016) 116.
[11] P. Glorioso, H. Liu, and S. Rajagopal, Global anomalies, discrete symmetries, and hydrodynamic effective actions, arXiv:1710.03768.
[12] A. Vilenkin, Quantum field theory at finite temperature in a rotating system, Phys. Rev. D **21**, 2260 (1980).
[13] V. E. Ambruş and E. Winstanley, Rotating quantum states, Phys. Lett. B **734**, 296 (2014).
[14] V. E. Ambrus and E. Winstanley, Rotating fermions inside a cylindrical boundary, Phys. Rev. D **93**, 104014 (2016).
[15] M. N. Chernodub and S. Gongyo, Interacting fermions in rotation: Chiral symmetry restoration, moment of inertia and thermodynamics, J. High Energy Phys. 01 (2017) 136.
[16] M. N. Chernodub and S. Gongyo, Effects of rotation and boundaries on chiral symmetry breaking of relativistic fermions, Phys. Rev. D **95**, 096006 (2017).
[17] M. N. Chernodub and S. Gongyo, Edge states and thermodynamics of rotating relativistic fermions under magnetic field, Phys. Rev. D **96**, 096014 (2017).
[18] S. Ebihara, K. Fukushima, and K. Mameda, Boundary effects and gapped dispersion in rotating fermionic matter, Phys. Lett. B **764**, 94 (2017).
[19] A. Avkhadiev and A. V. Sadofyev, Chiral vortical effect for bosons, Phys. Rev. D **96**, 045015 (2017).
[20] N. Yamamoto, Photonic chiral vortical effect, Phys. Rev. D **96**, 051902 (2017).
[21] V. A. Zyuzin, Landau levels for an electromagnetic wave, Phys. Rev. A **96**, 043830 (2017).
[22] A. D. Dolgov, I. B. Khriplovich, A. I. Vainshtein, and V. I. Zakharov, Photonic chiral current and its anomaly in a gravitational field, Nucl. Phys. **B315**, 138 (1989).
[23] I. Agullo, A. del Rio, and J. Navarro-Salas, Electromagnetic Duality Anomaly in Curved Spacetimes, Phys. Rev. Lett. **118**, 111301 (2017).
[24] M. G. Calkin, An invariance property of the free electromagnetic field, Am. J. Phys. **33**, 958 (1965).
[25] H. Lipkin, Existence of a new conservation law in electromagnetic theory, J. Math. Phys. **5**, 696 (1964).
[26] T. W. B. Kibble, Conservation laws for free fields, J. Math. Phys. **6**, 1022 (1965).
[27] T. G. Philbin, Lipkin's conservation law, Noether theorem, and the relation to optical helicity, Phys. Rev. A **87**, 043843 (2013).
[28] S. Deser and C. Teitelboim, Duality transformations of Abelian and non-Abelian gauge fields, Phys. Rev. D **13**, 1592 (1976).
[29] R. P. Cameron and S. M. Barnett, Electric-magnetic symmetry and Noether theorem, New J. Phys. **14**, 123019 (2012).
[30] Y. Tang and A. E. Cohen, Optical Chirality and Its Interaction with Matter, Phys. Rev. Lett. **104**, 163901 (2010).
[31] K. Y. Bliokh, Y. S. Kivshar, and F. Nori, Magnetoelectric Effects in Local Light-Matter Interactions, Phys. Rev. Lett. **113**, 033601 (2014).
[32] F. Alpeggiani, K. Y. Bliokh, F. Nori, and L. Kuipers, Electromagnetic Helicity in Complex Media, Phys. Rev. Lett. **120**, 243605 (2018).
[33] M. Elbistan, Optical helicity and Hertz vectors, Phys. Lett. A **382**, 1897 (2018).
[34] M. Elbistan, P. A. Horvathy, and P.-M. Zhang, Duality and helicity: The photon wave function approach, Phys. Lett. A **381**, 2375 (2017).
[35] R. P. Cameron, S. M. Barnett, and A. M. Yao, Optical helicity, optical spin and related quantities in electromagnetic theory, New J. Phys. **14**, 053050 (2012).
[36] B. R. Iyer, Dirac field theory in rotating coordinates, Phys. Rev. D **26**, 1900 (1982).
[37] O. Levin, Y. Peleg, and A. Peres, Unruh effect for circular motion in a cavity, J. Phys. A **26**, 3001 (1993); V. A. De Lorenci and N. F. Svaiter, A rotating quantum vacuum, Found. Phys. **29**, 1233 (1999).
[38] P. C. W. Davies, T. Dray, and C. A. Manogue, The rotating quantum vacuum, Phys. Rev. D **53**, 4382 (1996).